



# A review on magnetic abrasive finishing

Cheng Qian<sup>1</sup> · Zenghua Fan<sup>1,2</sup> · Yebing Tian<sup>1,2</sup> · Yanhou Liu<sup>1,2</sup> · Jinguo Han<sup>1,2</sup> · Jinhui Wang<sup>1,2</sup>

Received: 1 July 2020 / Accepted: 4 November 2020 / Published online: 25 November 2020  
© Springer-Verlag London Ltd., part of Springer Nature 2020

## Abstract

Magnetic abrasive finishing (MAF) has attracted much attention as an advanced nano-finishing technology in achieving high-quality surface for finishing superalloys, composites, and ceramics. This paper provides a comprehensive review on MAF process which is mainly organized by different six sections, including MAF principles, magnetic abrasive preparation, MAF tools, MAF modeling and simulation, MAF characteristics, and challenges and future directions. The principle of MAF for internal workpiece and flat workpiece is mainly introduced. Magnetic preparation methods, including simply mixing method, bonding method, sintering method, gas atomization, and rapid solidification method, are described in detail. The design of MAF tools for outer surface and inner surface is summarized. It also covers some models and simulations to predict optimal processing parameters. Force measurement and material removal mechanism to explore the MAF processes are performed. Finally, challenges and future directions are provided. This review is beneficial to researchers and practitioners in the MAF-related fields.

**Keywords** Magnetic abrasive finishing · Abrasive preparation · Finishing tools · Modeling · Simulation

## 1 Introduction

High-performance parts characterized by ultra-precision complex surface and functional micro-/nano-surface layers are mainly used in aerospace industry, semiconductors, and medical devices [1]. High-quality surface is usually achieved by variable traditional approaches such as grinding [2], lapping [3], and honing [4]. The above traditional processes are restricted from the following aspects: difficulties in fixture design according to different workpiece shapes and sizes, the limitation of advanced engineering materials, the low efficiency, and accuracy [5]. Nowadays, some untraditional nano-finishing technologies, including abrasive flow machining (AFM), magnetic field-assisted finishing (MFAF), elastic emission machining (EEM), and ion beam machining (IBM), are proposed for fabrication of precision components to solve defects of traditional polishing [6]. MFAF is generally

divided into magnetic abrasive finishing (MAF), magnetic abrasive flow finishing (MAAF), magnetorheological finishing (MRF), magnetorheological jet polishing (MJP), etc. The main difference of the above processes lies in finishing media divergence, using bonded or unbound abrasive and magnetorheological fluids, and flowing finishing media respectively. Comparison of finished surface obtained by various finishing processes mentioned above was summarized in Table 1 [7]. EEM [8] and IBM [9] work on the principal of removing atoms and molecules directly from the workpiece surface. Other processes perform the microchips through indentation and shearing of material. MFAF improves the final surface finish by deterministically controlling finishing force of the applied magnetic field.

MAF process has aroused great attention in finishing of composites [10], superalloys [11], and ceramics [12] for high-surface integrity. MAF is a flexible process without limitations in the size and shape of the workpiece including inner surfaces, outer surface, free-form surface, and complex curved surfaces [5]. A nanometer level surface is obtained by MAF within a few minutes which produce neither a deteriorated layer nor micro-cracks [13]. Controllability, self-adaptation and self-sharpness are outstanding characters of magnetic abrasive in MAF [14]. During the finishing process, a relative motion between the magnetic abrasive and the workpiece is formed to finish the workpiece. According to various finishing tasks, the designed MAF tool is easy to integrate with

✉ Yebing Tian  
tianyeb@sdu.edu.cn; tyb79@sina.com

<sup>1</sup> School of Mechanical Engineering, Shandong University of Technology, 266 Xincun West Road, Zibo, Shandong 255049, People's Republic of China

<sup>2</sup> Institute for Advanced Manufacturing, Shandong University of Technology, 266 Xicun West Road, Zibo 255049, People's Republic of China

**Table 1** Surface finish obtainable by various finishing processes [7]

S. No.	Finishing process	Workpiece	Ra value (nm)
1	Grinding	-	25–6250
2	Honing	-	25–1500
3	Lapping	-	13–750
4	Abrasive flow machining (AFM) with SiC abrasives	Hardened steel	50
5	Magnetic abrasive finishing (MAF)	Stainless steel	7.6
6	Magnetic Float Polishing (MFP) with CeO <sub>2</sub>	Si <sub>3</sub> N <sub>4</sub>	4.0
7	Magnetorheological finishing (MRF) with CeO <sub>2</sub>	Flat BK7 Glass	0.8
8	Elastic emission machining (EEM) with ZrO <sub>2</sub>	Silicon	< 0.5
9	Ion beam machining (IBM)	Cemented carbide	0.1

automated equipment such as milling machine, industrial robot to provide relative motion as a separate module [15, 16].

Based on the aforesaid need of a MAF process review, a critical review on various aspects of the MAF is provided to give a more a detailed overview of the technology. Sections of MAF principles, magnetic abrasive preparation, MAF tools, MAF modeling, MAF simulation, MAF characteristics, and challenges and future directions are included in the review. Major issues and performance improvement techniques are discussed in detail. Finally, the future scopes are discussed.

## 2 MAF principles

MAF process is defined as a technology by material removal, in such a way that workpiece's precision machining is performed through relative motion between magnetic abrasive and workpiece with the presence of a magnetic field in the finishing zone [17]. Magnetic abrasive is mainly composed of ferromagnetic particles and abrasive particles, in which a flexible magnetic abrasive brush (FMAB) is formed along the direction of the magnetic force lines [18, 19]. Various workpieces with cylindrical surface, internal surface, and free-form surface can be finished because of the formed flexible finishing tool [20, 21].

Some scholars developed MAF technology with different configurations based on the classic finishing principle. Yamaguchi et al. [22] reported the internal finishing of alumina ceramic components using a work rotation system, as shown in Fig. 1. The four small permanent magnets poles, which were arranged evenly on the circular yoke, generated the magnetic field needed for attracting the ferrous particles to gather on the inner surface of the tube. The diamond abrasive in the mixture performs micro-cut the inner surface of the tube when the tube was rotated at high speed. The vibration applied on the magnetic poles accelerated the movement of the finishing media, thereby leading to efficient surface finishing. Barman et al. [23] proposed the finishing of a flat workpiece surface using MAF, as shown in Fig. 2. The finishing tool was

made of a single permanent magnet to generate gradient magnetic field, in which the magnetic abrasive was condensed in the working gap to be a flexible brush. The material removal was achieved by adjusting rotational motion and translation motion.

Based on the MAF principles, additional ultrasonic vibration is used to achieve perfect and high-quality workpiece surface. Mulik et al. [24] employed ultrasonic vibration in the horizontal direction of the workpiece using an ultrasonic power, a piezoelectric transducer, and a horn device. A high-frequency electrical signal was generated by the ultrasonic power and transformed into the horizontal mechanical vibration by the transducer. Zhou et al. [25] adopted ultrasonic vibration module held the machine spindle to load ultrasonic vibration along the vertical of the workpiece.

## 3 Magnetic abrasive preparation

Magnetic abrasive has been commercialized and composed of ferromagnetic phase (carbonyl iron particle) and abrasive phase (silicon carbide, alumina, diamond), which plays a critical role in finishing process [26], as shown in Fig. 3. The

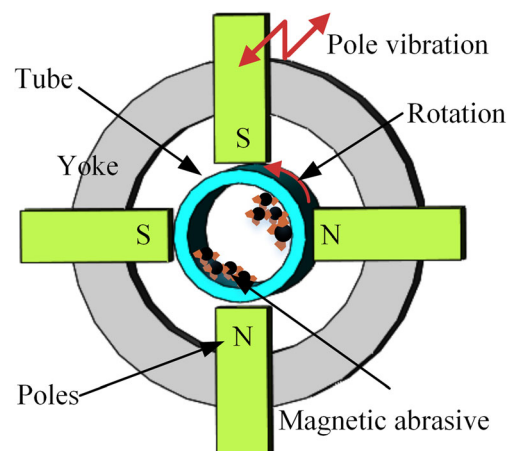


**Fig. 1** Finishing principle of internal workpiece [22]

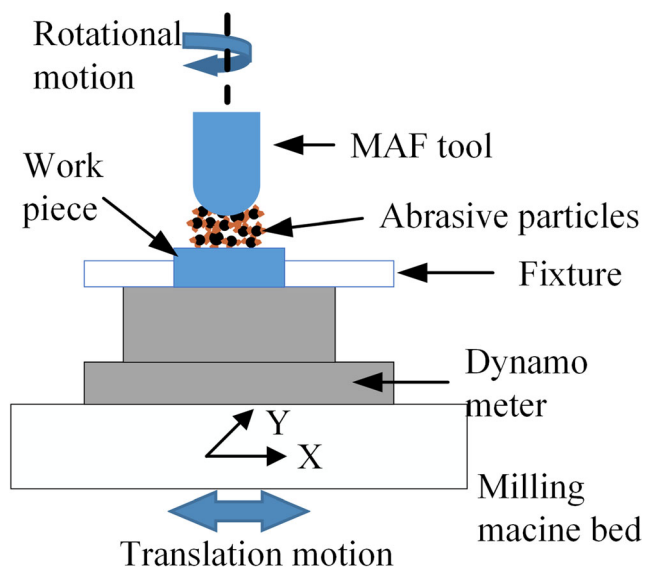


Fig. 2 Finishing principle of flat workpieces [23]

main function of ferromagnetic phase is to make magnetic abrasive generate strong magnetic pressure under the action of applied magnetic field. The volume fraction of ferromagnetic phase is vital to dominate magnetic pressure and finishing performance. The abrasive phase focused on material removal from the workpiece surface; therefore the hardness of the employed abrasive phase is higher than that of the workpiece [27].

Many magnetic abrasive preparation methods have been proposed, such as simply mixing method [28], bonding method [29], sintering method [30], gas atomization, and rapid solidification method [26]. Simply mixing method is to make the ferromagnetic phase and the abrasive phase by stirring in a certain proportion. Although the method is simple, magnetic abrasive is easily decomposed during the finishing process leading to low finishing efficiency [28, 31]. Bonding method by using binder to make ferromagnetic phase and abrasive

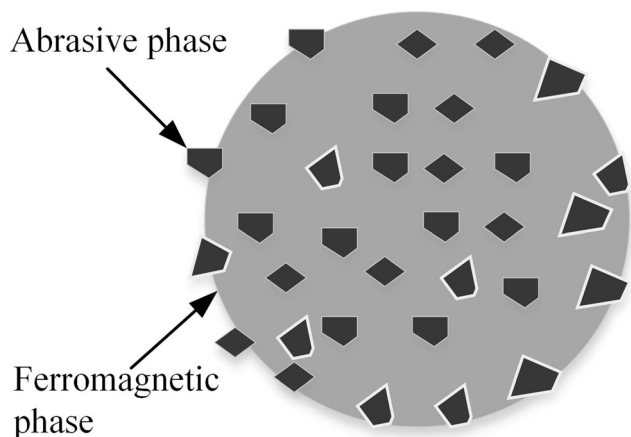


Fig. 3 Ideal structural model of a single magnetic abrasive [26]

phase mixed, the magnetic abrasive is gained after solidifying, crushing, and screening. Although the bonding method is characterized as low cost and relatively simple, the prepared magnetic abrasive is easily oxidized [14, 28]. The sintering method is employed to prepare magnetic abrasive through preparing, mixing, pressing, drying, sintering, crushing, and screening processes [32]. The prepared magnetic abrasive has several advantages of higher stability and longer working life, and the ferromagnetic phase and abrasive phase can be combined firmly [33, 34]. Under the action of gas atomization and rapid solidification method, the molten ferromagnetic phase and abrasive phase mixed fiercely. Magnetic abrasive is obtained after cooling, solidifying and screening processes [26]. To further improved preparation process, Gao et al. [35] presents a new gas-solid two-phase double-stage atomization with rapid solidification. Uniform composition, high cutting capacity, and long working life are outstanding features of prepared magnetic abrasive using the method.

Table 2 shows the finishing performance of various magnetic abrasives for different workpiece properties. Ingredients and proportions of magnetic abrasive are the main factors affecting the properties of abrasive. To further improve the performance of magnetic abrasive, Li et al. [27] presented a new magnetic abrasive, which was composed of base polymer, plasticizers, ferromagnetic particles, and abrasive particles. The change of the roughness reaching the maximum of 94.85% with the mass ratio of base polymer, ferromagnetic phase, and abrasive phase was 4:3:1. Fan et al. [39] developed an enhanced magnetic abrasive combining the intelligent shear thickening fluid (15 wt.%), carbonyl iron particles (42.5 wt.%), and silicon carbide particles (42.5 wt.%) through mechanical stirring. The surfaces roughness of 54 nm was achieved from an initial value of 1.17  $\mu\text{m}$  through finishing experiments for Ti-6Al-4 V workpiece.

## 4 MAF tools

MAF tools for finishing various workpieces with irregular shapes have been developed, such as cylindrical structures, internal structures, and free-form surface. Generally, the finished workpieces can be divided into two categories. One is the outer surface workpiece, and the other is the inner surface workpiece. Various finishing tools of MAF are discussed in detail.

### 4.1 Finishing tools for outer surface

Planar tools are suitable for finishing workpieces with complex curved surfaces and free-form surface because magnetic abrasive has the adaptability and fluidity to conform curved surfaces. As shown in Fig. 4, Kanish et al. [40] designed a MAF tool for flat surface finishing. The finishing process was performed by application of a magnetic field across the

**Table 2** Finishing performance of various magnetic abrasives

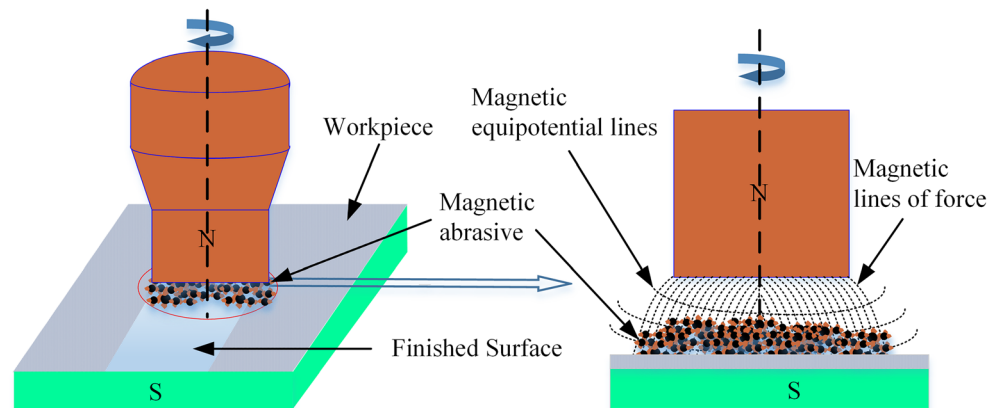
S. No.	Ingredients of magnetic abrasive	Proportions of magnetic abrasive	Preparation method	Workpiece	Surface roughness	Reference
1	The ferromagnetism iron particles, the alumina particles, and the lapin	Weight ratio (ferromagnetism iron: the alumina particles) = 4:1	Simply mixing method	Bass	2–0.4 $\mu\text{m}$	Chen et al. [28]
2	SiC abrasive, ferromagnetic particles, and a SAE30 lubricant	Weight ratio (ferromagnetic particles: SiC abrasive, SAE30 lubricant) = 4:1:0.6	Unbonding method	SKD11	0.677–0.038 $\mu\text{m}$	Chang et al. [14]
3	Iron particle particles, the alumina particles, and lubricant	Weight ratio (iron particle particles, the alumina particles) = 4:1	Bonding method	AISI304 stainless steel	2.572–0.008 $\mu\text{m}$	Yang et al. [36]
4	SiC abrasive and ferromagnetic particles	Weight ratio (ferromagnetic particles: SiC abrasive) = 4:1	Sintering method	SS304	0.240–0.049 $\mu\text{m}$	Shukla et al. [37]
5	CBN/Fe-based spherical magnetic abrasive	The following Proportions (in wt.%): 9.4 Si, 5.0 Ti, 5.8 Ni, 0.5 Cr, 2.0 B, balance Fe	Gas atomization and rapid solidification method	Ti-6Al-4 V	0.543–0.043 $\mu\text{m}$	Qin et al. [38]

working gap between the workpiece surface and the rotating magnetic pole. Due to the existence of magnetic lines of force and magnetic equipotential lines, magnetic abrasive was pressed tightly on the surface of the workpiece, which caused micro-cutting when the pole rotated. Du et al. [11] developed a MAF tool for finishing nickel-based superalloy GH4169 and drawled a conclusion that the surface roughness value reduced significantly and the surface morphology became smoother, the processing efficiency was improved by 50 %. The above-mentioned magnetic field generating tools were placed on the upper end of the workpiece. The magnetic field lines only formed closed loop around the permanent magnet and do not penetrate the workpiece. As a result, the generated flexible magnetic brush cannot tightly press the workpiece, which affects the processing effect. To overcome the weakness, Kwak et al. [41] installed a permanent magnet at the opposite side of the workpiece to increase the magnetic flux density. It was verified by experiments that the finishing effect of the tool with the permanent magnet was better than that without the permanent magnet. Kala et al. [42] presented a novel tool using two permanent magnets distributed on the upper and lower surfaces of the workpiece to further enhance magnetic flux density, and the maximum magnetic flux density was 0.3 T.

MAF tools integrated with multi-pole are developed for outer surface finishing. Laroux [43] designed a MAF tool for deburring of cylindrical surface, as shown in Fig. 5. A pair of permanent magnetic poles with a 180° distribution was designed. The magnetic abrasive was filled between the outer surface of the workpiece and the magnetic poles. Sato et al. [44] designed a double-magnet apparatus as shown in Fig. 6, which consisted of two parallel shafts with neodymium ring magnets attached to each end. One of the shafts was driven by a spindle motor and connected to the other shaft by spur gears. The whole tool was mounted on a milling machine. Material removal was achieved by the relative movement between magnetic abrasive and the workpiece. Fan et al. [45] investigated a novel finishing tool as shown in Fig. 7, which was mainly composed of four magnetic poles. The finishing tool was mounted on a four-axis CNC machine center. Magnetic abrasive could form a flexible brush in the finishing area under the action of four magnetic poles. A relative movement was generated by tool rotation and worktable movement, causing material to be removed by magnetic brush. Tian et al. [46] investigated magnetic abrasive finishing of Ti-6Al-4 V using a round tray, a baffle, and 64 poles. The workpiece was connected to the spindle. The surface roughness of 0.073  $\mu\text{m}$  was achieved from the initial 1.195  $\mu\text{m}$ .

In order to explore the forming behavior of FMAB, the researchers transformed permanent magnets into electromagnets, which can adjust the intensity of the magnetic field in the finishing area by changing the magnitude and frequency of the applied voltage. Chang et al. [14] investigated surface

**Fig. 4** Schematic view of MAF process for plane surfaces [40]



finishing of the cylindrical workpiece experimentally. A cylindrical workpiece was inserted in the gap between the two electromagnetic poles. Magnetic abrasive was filled in the gap between the workpiece and the electromagnetic pole. Magnetic abrasive exhibited a density brush because of the existence of electromagnetic field and adhered closely to the outer surface of the cylinder. A relative friction was generated by rotating the workpiece and controlling the axial vibration. Jain et al. [47] applied the electromagnetic coil around magnetic yoke to form magnetic poles. An orthogonal array  $L_9(3^4)$  was performed to study the influence of applied DC voltage to the electromagnet, working gap, rotational speed of electromagnet, and abrasive size on the surface quality. The voltage and working gap were the most significant parameters changing surface roughness. Xie et al. [48] studied on finishing tools using a coil which was supplied with AC power. The workpiece was placed on the upper part of the coil. A surface roughness of 5052 aluminum alloy plate was improved from  $R_a$  318 to 3 nm in 15 min.

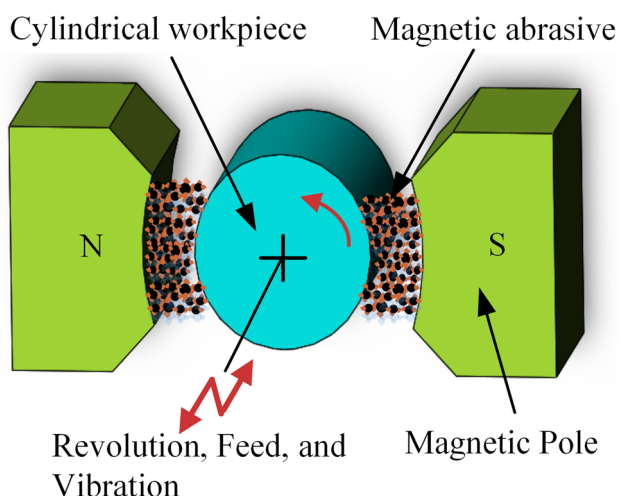


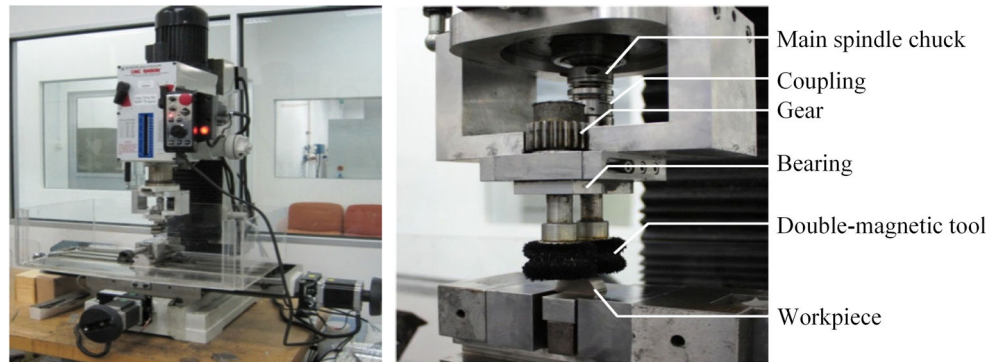
**Fig. 5** Schematic principle of the cylindrical surfaces [43]

#### 4.2 Finishing tools for internal surface

The design principle of finishing tools for internal surface which is consistent with principle for designing outer surface is to use magnetic field to absorb magnetic abrasive to form FMAB, and the surface finishing is performed by squeezing, sliding, and grinding the workpiece surface. However, the main difference between two design methods is the position of the magnetic field generator relative to the finished target surface, where the magnetic field generator for internal surface is set on the outside due to the feature that magnetic field can penetrate non-magnetic materials [49].

Finishing tools for internal surface were mainly developed by Shimamura and Yamaguchi [50, 51]. Yamaguchi [52, 53] developed a MAF tool based on a stationary pole system. Figure 8 shows a schematic of finishing process for internal surface. Magnetic abrasive was conglomerated at the finishing zone applying an electromagnetic field, and then the finishing force was generated against the inner surface of the tube. The relative friction between the workpiece internal surface and flexible brush caused by the rotation and vibration of tube at a high speed removed the material. The inner surface of the tube became smooth accordingly. Yamaguchi et al. [54] developed a novel finishing equipment, in which electromagnetic coils facing each other in a parallel circuit generated an alternating magnetic field. Magnetic abrasive inside the workpiece was controlled by the formed alternating magnetic field. Sato et al. [55] proposed a finishing setup by applying two electromagnets placed at 90 angles. The abrasive was attached to the inner surface of the workpiece tightly when the current was applied. The workpiece with rotation driven by the motor and axial vibration achieved by a crank mechanism connected to the motor caused a relative motion resulting in surface cut. Singh et al. [56] also use mutually perpendicular electromagnetic poles applied DC power as the magnetic field generator of the finishing setup. For the relative motion, the desired radial vibration of the magnetic field generator was generated by an eccentric, a gear box, and a motor. Workpiece was

**Fig. 6** The double-magnet MFAF apparatus [44]



clamped on the chuck connected to the motor so as to provide rotation. For the above-mentioned electromagnetic magnetic field generator can also be converted into permanent magnetic. Wang et al. [57] developed a finishing setup, as shown in Fig. 9 (a). The relative motion was created by the magnetic pole rotating system. Figure 9 (b) shows the schematic diagram of the magnetic field generator. For exploring higher finishing efficiency and magnetic field strength, the optimized processing conditions were regulated by changing axial vibration [22], placement angles of magnetic poles [58], and distributions of magnetic poles [59].

## 5 MAF modeling and simulation

### 5.1 Prediction modeling of surface roughness

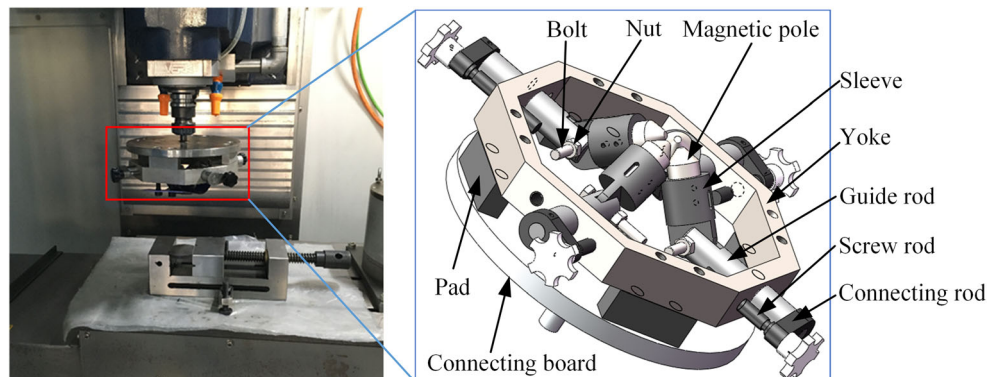
The surface roughness is a vital parameter to evaluate finishing ability. By establishing a prediction model of workpieces' surface roughness, influences of the abrasive size, spindle speed, machining gap, and magnetic flux density on roughness changes are explored to achieve the objective of optimizing finishing parameters, which contributes to provide theoretical guidance [60, 61]. According to the measuring mechanism of the atomic force microscope (AFM), roughness values can be calculated by using the following equation [62]:

$$S_q = \sqrt{\frac{1}{PQ} \sum_{i=0}^{P-1} \sum_{j=0}^{Q-1} (z(x_i, y_j))^2} \quad (1)$$

where  $S_q$  is the roughness value;  $P$  and  $Q$  are the points number along  $x$  and  $y$  directions, respectively, after meshing the finishing surface; and  $z(x_i, y_j)$  is the position change of corresponding grid  $(x_i, y_j)$ .

Jain et al. [63] investigated the surface roughness model which computed center-line average using non-uniform surface profiles exhibiting height distribution of Gaussian. Numerical experiments were performed to study the effect of flux density, height of working gap, size of magnetic abrasive particles, and rotational speed of magnetic pole on the surface quality. The results showed that the roughness value is inversely proportional to the magnetic flux density, magnetic abrasive particle size and the rotating speed of flexible magnetic abrasive brush, and directly proportional to the working gap. Kajal et al. [64] provided the theoretical model to predict the final surface roughness during internal MAF of a revolver based on the assumption that an initial uniform surface profile with roughness peaks running circumferentially in the inner cylindrical surface with the abrasive particles cutting these peaks along a helical path. Different parameters on the percentage improvement in roughness were studied, including rotational speed, volume percent of abrasive particles,

**Fig. 7** Experimental equipment with four magnetic poles [45]



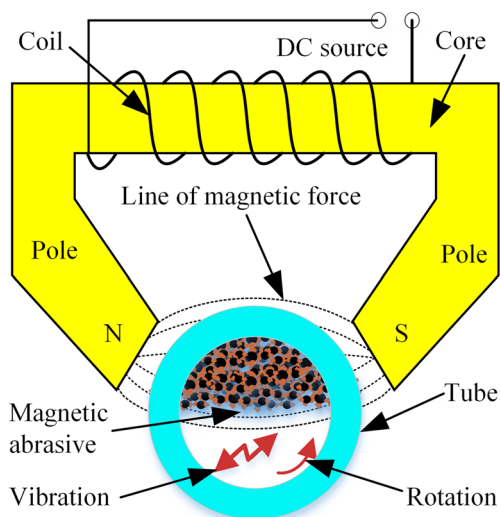


**Fig. 8** Schematic of internal MAF process using a stationary pole system [53]

working gap, abrasive mesh size, and feed rate. Kala et al. compared finishing characteristics of two paramagnetic materials using double disc magnetic abrasive finishing [65] and then proposed a mathematical model for double disk to predict the surface roughness of stainless-steel workpiece [66]. Experiments were performed to validate the mathematical model. The established model was built using Lorentz force equation, amperes law, and statistical approach. The surface roughness was modeled as a function of working gap, abrasive mesh number, percentage weight of abrasive, rotational speed and feed rate. According to the simulation data, the percentage change in surface roughness increases with the decrease of feed speed. The percentage change in surface roughness was inversely proportional to working gap and abrasive weight percentage and directly proportional to abrasive mesh number. Spindle speed of 400 rpm was a critical value regarding the percentage change in surface roughness.

### 5.2 Simulation of abrasive trajectory

The kinematic model of the abrasive is established to simulate the abrasive trajectory during MAF processes. Parameters of feed speed of workpiece, spindle rotational speed, amplitude, and frequency of vibration are included in the established kinematic model [49]. The trajectories are varied by changing the parameters which affect the finishing efficiency. The choice of motion parameters is achieved for different workpieces using the model.

Yun et al. [67] explored the method to improve the efficiency of MAF for the inner surface of alumina ceramic tubes by changing the trajectory of a magnetic abrasive brush. The kinematic model was built using parameters including the radius of workpiece, relative angular speed, and vibration frequency, as described in Eq. (2). Where  $x, y, z$  is three-dimensional coordinate point of magnetic abrasive,  $R$  is the radius of workpiece,  $\omega$  is the rotation angle of FMAB  $t$  is finishing time,  $V$  is the speed of axial feeding,  $A$  is the amplitude of vibration, and  $f$  is the vibration frequency.

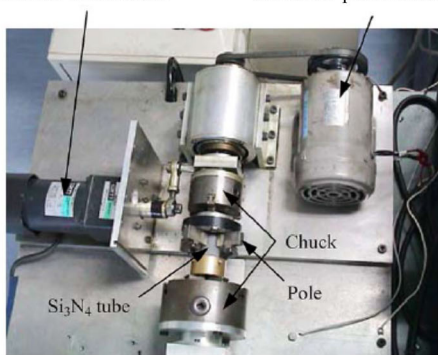
$$\begin{cases} x = R \sin(\omega t) \\ y = R \cos(\omega t) \\ z = V\omega t / 2\pi + A \sin(2\pi f t) \end{cases} \quad (2)$$

Effects of vibration frequency and workpiece speed on trajectory of the magnetic abrasive brush were studied, as shown in Fig. 10. Trajectory motion simulations were achieved by setting process parameters of 1000 r/min workpiece rotational speed, 2 mm/s feeding speed, and 5 mm amplitude. The frequency and workpiece speed improved the processing in varied degrees and had different finishing characteristics of the surface roughness and material removal.

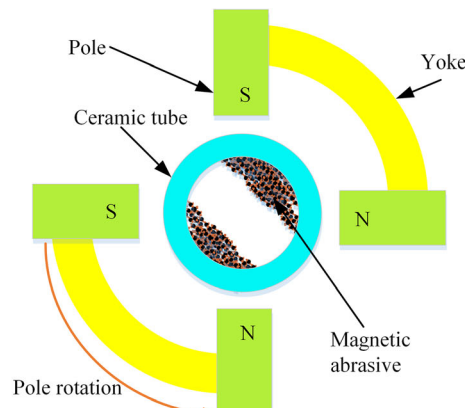
Jiao et al. [68] calculated the trajectory to elevate the surface quality of plane magnetic abrasive finishing. Abrasive trajectory can be predicted combining revolution motion of magnetic abrasive brush, the pole rotation motion, and linear

**Fig. 9** Experimental setup. (a) External view. (b) Schematic of magnetic field generator [57]

Motor for pole vibration in the Direction of tube axis      Motor for pole rotation



(a)



(b)

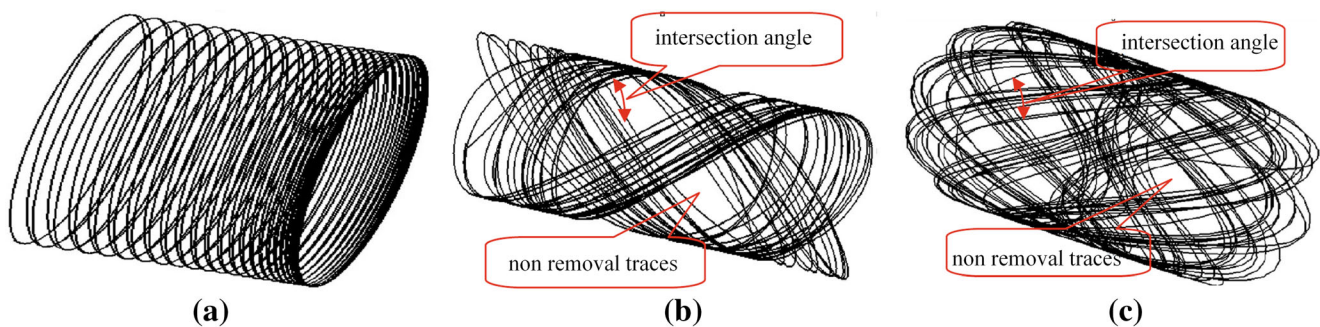


**Fig. 10** Effects of frequency on the magnetic abrasive trajectory. (a) Frequency of 0 Hz, (b) frequency of 10 Hz, and (c) frequency of 30 Hz [68]

reciprocating motion of workpiece to investigate finishing results. The experiments showed that the plane homogeneity and surface quality were improved in varying degrees by changing the polishing trajectory. The simulation of motion trajectory analysis was consistent with the experimental results. Li et al. [27] studied the trajectory of an abrasive particle for internal surface finishing. The three-dimensional coordinates of the magnetic abrasive were obtained based on a function of the angular velocity of the magnetic poles, the radius, and the angular velocity of the cam to simulate the abrasive motion trajectories. The abrasive formed the complex motion relative to the workpiece.

### 5.3 Simulation of magnetic field

The magnetic intensity determines the finishing efficiency directly. The magnetic field simulation of the poles is carried out to explore the field strength and gradient in various tools using Maxwell software. Jayswal et al. [69] dealt with the effect of a slot made in the electromagnet on the forces and surface quality. It was found that force got enhanced around the slot, and the direction of force changes in the area under the slot. High-surface finishing can be achieved with slot in a shorter time. Srinivas et al. [70] explored the effects of magnet shape on the

machining of workpiece by simulation. Magnetic poles with four shapes, including fan-shaped magnetic poles, arc-shaped magnetic poles, ring-shaped magnetic poles, and two magnetic poles, were simulated to predict the magnetic field strength. The arc-shaped magnet showed the maximum magnetic field intensity. Fan et al. [45] designed a novel finishing tool, in which magnetic field generator integrated with four permanent magnets as a tool to achieve alternating magnetic regions. Two kinds of distribution of four magnetic poles, N-N-S-S and N-S-N-S, were performed using Maxwell analysis as shown in Fig. 11. Two closed loops and four closed loops were obtained based on the two distributions, respectively. The four closed loops formed four protrusions contributing to the improvement of finishing efficiency. Simulation of the magnetic field generating tool is regarded as the real finishing environment, resulting in a large error.

In order to explore the optimal shape of the magnetic pole to obtain the highest processing quality, various approaches are performed on the magnetic pole design. Zhao et al. [71] investigated the slotting size of magnetic pole through numerical simulation and experiments. The results showed that the rectangular pole contributes to a better magnetic field distribution than the V-shaped groove and the funnel-shaped groove. Yin et al. [72] confirmed that the slotted tool obtained a better

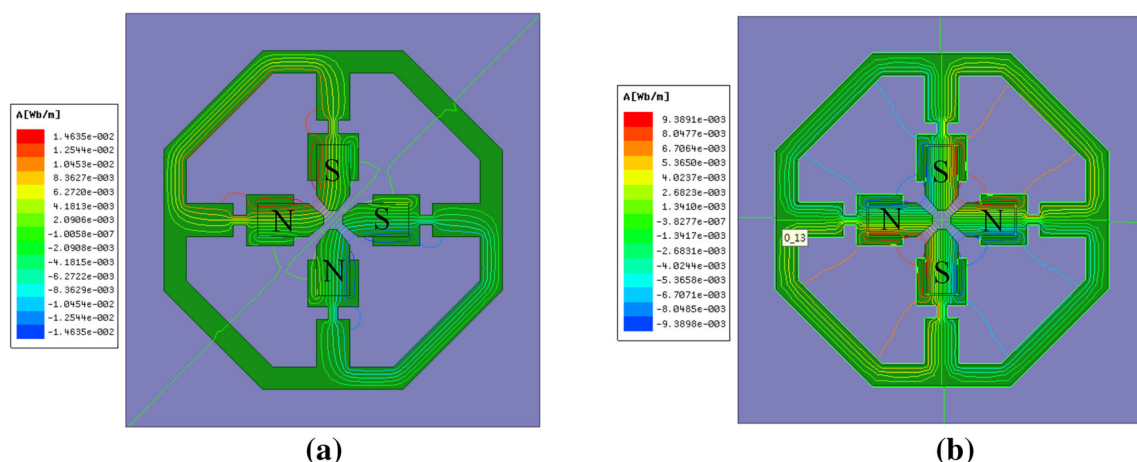


**Fig. 11** Distributions of four magnetic poles. (a) N-N-S-S arrangement. (b) N-S-N-S arrangement [45]



surface than the non-slotted tool. Liu et al. [73] investigated the influence of taper magnet and the rectangular slot magnet pole on the magnetic field distribution. Zhao et al. [74] simulated the distributions of magnetic field lines on the surface of the tapered magnetic pole and the spherical magnetic pole. Zhang et al. [75] explored the end slotting approaches of a single magnetic pole using tian word slot and mi word slot. The novel design can be employed to prevent the local accumulations of abrasive, which helped to ensure the abrasive fluidity and increase the magnetic flux density. However, tian word slot magnetic pole was more efficient in the prophase finishing processes because of the strong flux density on pole end.

#### 5.4 Simulation of temperature

The surface quality has a greater dependency on temperature of the target surface during the micro finishing due to the rubbing action of magnetic abrasive particles. Mishra et al. [76] performed the simulation of temperature range during the process of MAF using finite element-based ANSYS software. Transient thermal analysis of workpiece domain was performed to predict the temperature rise due to frictional heat flux. The simulation results were slightly higher than the experimental results because of the heat loss in plastic deformation and microchips. Wang et al. [77] evaluated the temperature during MAF of Mg alloy bars using experimental data. Experiments were conducted at three different temperatures of  $-120$ ,  $24$ , and  $112^{\circ}\text{C}$ . By comparing the improvement of roughness, the optimum temperature of  $24^{\circ}\text{C}$  was obtained. Singh et al. [78] analyzed the raise in temperature using the developed Buckingham- $\pi$  dimensional model during MAF processes. The predicted temperature had good agreement with 7.31% average error in respect to the experimental results.

#### 5.5 Simulation of finishing process

The simulation of material removal mechanism contributes to explain the physical essence of finishing process and guides the actual processing. Mosavat et al. [62] simulated the process of finishing monocrystalline silicon wafers using

smoothed particle hydrodynamics (SPH) method. The material removal and reduction in surface roughness value increased with increasing abrasive size, workpiece rotational speed, and decreasing machining gap. Figure 12 showed the simulation resulted at different speeds. The coupled algorithm of SPH/FEM (the finite element method) was employed to simulate the surface finishing of silicon wafers. In addition, the material removal mechanism in wafers was investigated using AFM [79]. Jayswal et al. [80] developed a finite element model of the MAF process to evaluate the distribution of magnetic forces on the workpiece surface. A theoretical model for material removal and surface roughness was proposed to verify the magnetic abrasive behavior. Madhab et al. [81] established a finite element model for the simulation of plane MAF. The model was simplified as an axisymmetric configuration. A theoretical model for stock removal was developed by considering indentation depth of abrasive particles on workpiece surface.

### 6 MAF characteristics

#### 6.1 Forces acting on a ferromagnetic particle

Figure 13 shows the schematic diagram of forces acting on a ferromagnetic particle. The magnetic abrasive is mainly suffered by  $F_x$  along the magnetic equipotential line and  $F_y$  along force line under the action of a magnetic field, in which the directions of the  $F_y$  can be changed according to alternating magnetic pole's direction. The resultant force  $F$  is shown in Eq. (3). [12]

$$\begin{cases} F_x = V\chi\mu_0 H \left( \frac{\partial H}{\partial x} \right) \\ F_y = V\chi\mu_0 H \left( \frac{\partial H}{\partial y} \right) \\ F = F_x + F_y \end{cases} \quad (3)$$

where  $V$  is the volume of the ferromagnetic particle,  $\chi$  is the susceptibility of the ferromagnetic particles,  $\mu_0$  is the magnetic permeability in vacuum,  $H$  is magnetic field strength, and

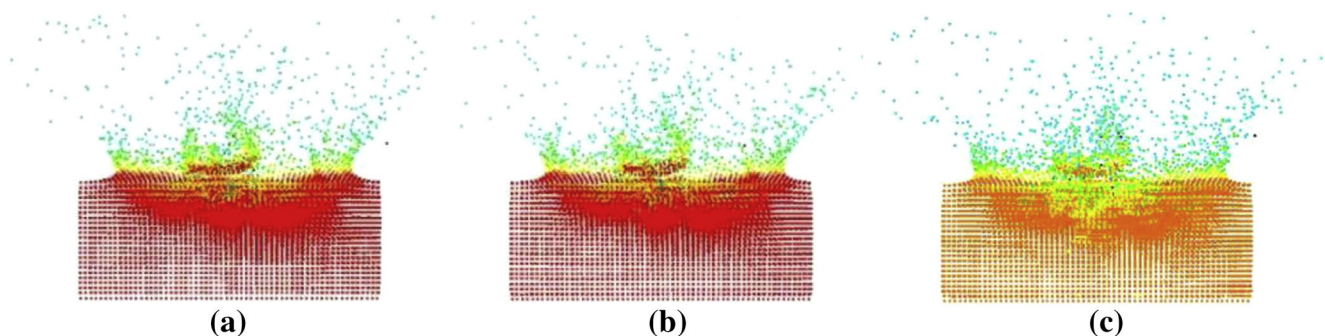
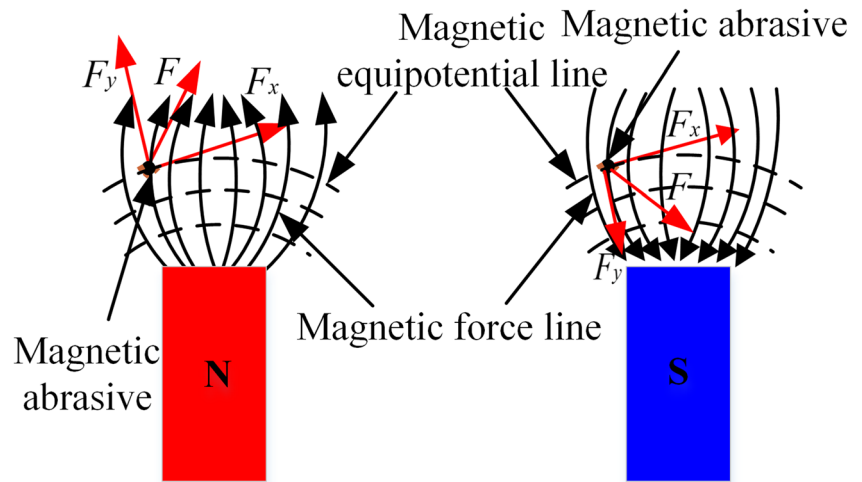


Fig. 12 Simulation of finishing process at different rotational speed. (a) 800, (b) 1500, and (c) 2000 rpm [79]

Fig. 13 Schematic diagram of magnetic force [12]



$\partial H/\partial x$  and  $\partial H/\partial y$  are the gradient magnetic field strength in the  $x$  and  $y$  directions, respectively.

Figure 14 shows the finishing forces acting an external cylindrical surface, which is divided into the normal force,  $FN$ , along the  $N-N$  direction, and the tangential force,  $FT$ , along the  $T-T$  direction [82].

$$\begin{cases} FN = FX\cos\theta + FY\sin\theta \\ FT = -FX\sin\theta + FY\cos\theta \end{cases} \quad (4)$$

where  $\theta$  represents the placement angle determined by the arrangement of magnetic poles and the location of the ferromagnetic particle and  $FX$  and  $FY$  can be calculated using Eq. (3).

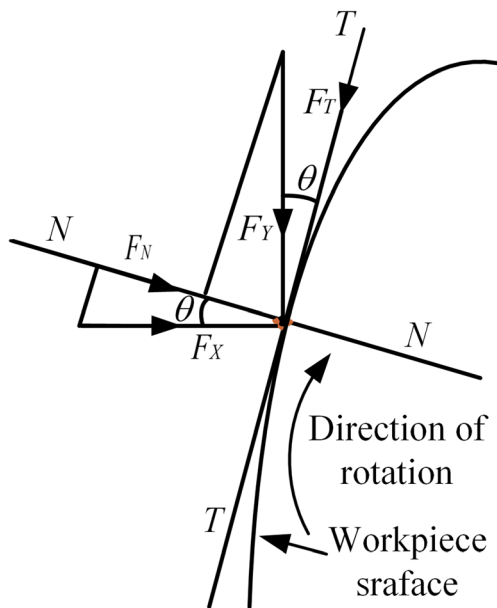


Fig. 14 Schematic diagram of magnetic abrasive acting on the external cylindrical surface [82]

In the finishing process, magnetic abrasive filled in the machining gap along the direction of magnetic force lines, thus forming a MFAB. The magnetic pressure  $P$  exerted by the magnetic abrasive on the workpiece surface is related to the magnetic flux density, as shown in Fig. 15. The pressure  $P$  acting on the external cylindrical surface is expressed as [83]

$$P = \frac{B^2}{4\mu_0} \times \frac{3\pi(\mu r - 1)\omega}{3(2 + \mu r) + \pi(\mu r - 1)\omega} \quad (5)$$

where  $B$  is the magnetic flux density,  $\mu r$  is the relative magnetic permeability of ferromagnetic, and  $\omega$  is the volume percentage of the ferromagnetic particles in magnetic abrasive.

### 6.2 Mensuration of forces during MAF process

Kim and Choi [84, 85] established mathematical models of the finishing pressure during magnetic finishing of free-form

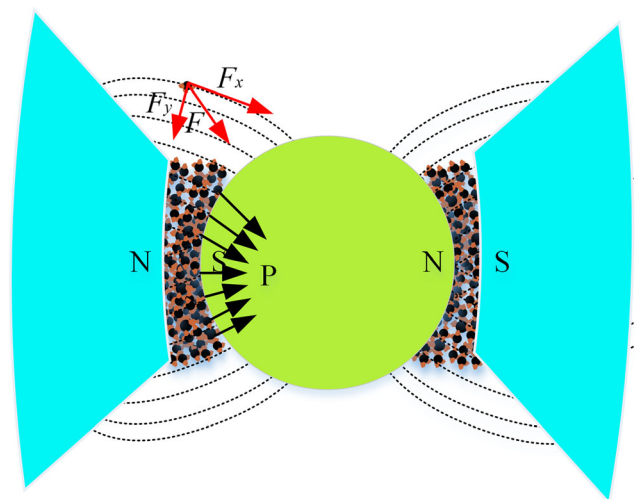


Fig. 15 Sketch of force analysis of magnetic abrasive [83]

surfaces. The finishing pressure was less than  $50 \text{ KN/m}^2$ , and the finishing force varied from 16 to 75 N. Mori et al. [86] developed the theoretical equation for normal and tangential force during the finishing process. They observed that the normal force for different magnetic abrasive weight percentage varied from 0 to 20 N. Singh et al. [87] designed and fabricated a test platform using force transducer (ring dynamometer) with 0.5 N resolution. Further experiments were performed to explore forces acting a MAF process [88]. The normal and tangential finishing forces were important parameters which influenced workpiece surface roughness. Kanish et al. [18] investigated the finishing forces during the finishing of SS316L. The normal and tangential forces were measured using Kistler dynamometer and a charge amplifier. The experimental result showed that the higher voltage (22 v) and lower machining gap (1.5 mm) make a higher normal force and tangential force. Ganguly et al. [19] measured the normal finishing forces to eliminate interference from other factors, such as sample mount, slurry and sample. The tangential force was the average value of the tangential finishing force of multiple reciprocating cycles. The effect of various processing parameters like the working gap, the size of the ferromagnetic iron particles, and translation velocity of lateral forces were explored. It was found that the normal and tangential finishing force had an inverse relationship with both iron particle size and working gap.

### 6.3 Material removal mechanism

Material removal rate (MRR) is one of the key research issues for MAF process, in which the finishing efficiency is predicted based on the given input process parameters. Figure 16 showed the schematic illustration of the material removal [45]. Optimal processing parameters are obtained for a new task previously based on the prediction of MRR, which helps to reduce or eliminate multiple experiments. Therefore, the predicative precision for MRR is vital for adjusting processing parameters automatically. Generally, MRR is mainly established by the following methods, including Preston equation and Archard wear equation.

Preston equation was proposed as one of the earliest MRR models for lapping of glass plates. The Preston equation, as an empirical formula in grinding and polishing, has been widely used in engineering. It classifies all factors that affect material removal rate except the speed and pressure of the abrasive on the surface of the workpiece into a proportional constant. The formula is described as follows [89]:

$$MRR = KPV \quad (6)$$

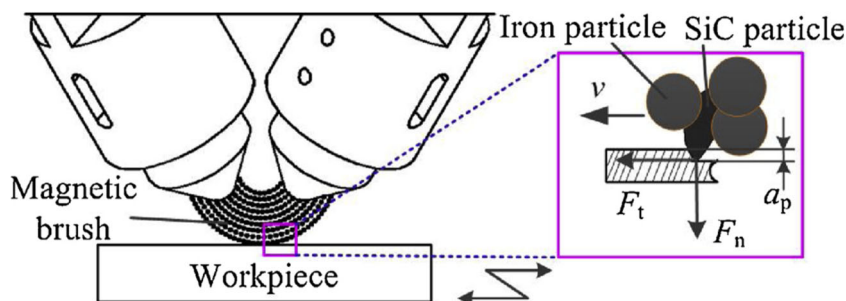
where  $K$  is the Preston coefficient,  $P$  is the pressure acting on workpiece surface, and  $V$  is the relative velocity between the brush and workpiece surface. The Preston coefficient is related to the chemical composition of the medium, the type of magnetic abrasive (size, shape, hardness), material properties of the workpiece, etc. The coefficient is modified through extensive experiments and expressed as [90, 91]:

$$K = k \left[ E^{4/5} / (KcH0^2) \right] \quad (7)$$

where  $k$  is the correction factor,  $E$  is Young's modulus,  $Kc$  is the fracture toughness, and  $H0$  is the Knoop hardness.

Workpiece pressure is mainly composed of hydrodynamic pressure, magnetization pressure and pressure generated by gravity [92, 93]. In general, the pressure caused by gravity is not considered because gravity pressure is negligible relative to hydrodynamic pressure and magnetization pressure. Wani et al. [94] and Li et al. [58] calculated MRR model only considering the magnetizing pressure applying Eq. (5). For MFAF with liquid, the hydrodynamic pressure is essential for the established MRR model. Zhang et al. [95] established a two-dimensional parabolic geometry of finishing process, and the hydrodynamic pressure was calculated based on geometrical relationship and Sommerfeld boundary condition in Reynolds equation. Chen et al. [96] further extended the boundary conditions of Reynolds equation to found the MRR model in two-dimensional. Li et al. [97] obtained the hydroxamic pressure according to Bingham model and the theory of hydrokinetics. Relative velocity should be calculated after the Preston coefficient, and pressure parameters were obtained. Relative velocity is usually a function of rotation

Fig. 16 Schematic illustration of the material removal [45]



speed, feed speed of workpiece, vibration amplitude, etc. Calculation method of relative velocity can be divided into two methods. One is to synthesize directly the abrasive velocity based on the partial velocity [98], and the other method is to calculate abrasive trajectory (Section 5.2 Simulation of abrasive trajectory) and then perform differentiation the time [99]. The above reference used the ferromagnetic phase and the abrasive phase as a whole to calculate MRR without considering the interaction of two different particles. Kum et al. [100] proposed the model considering the interaction of carbonyl iron particles and abrasives, and the Preston equation was transformed into Eq. (8). The model had been verified by experiments with a double-magnet MFAF process, and the result showed that the theoretical trend of the model was consistent with the experimental data, where  $K_{CI}$  and  $K_{abr}$  are the removed factors for active carbonyl iron particles and abrasives, respectively;  $N_{CI}$  and  $N_{abr}$  are the number of active carbonyl iron particles and abrasives respectively; and  $\Delta MRR_{CI}$  and  $\Delta MRR_{abr}$  are the MRR per active carbonyl iron particles and abrasives, respectively.

$$MRR = K_{CI} \cdot N_{CI} \cdot \Delta MRR_{CI} + K_{abr} \cdot N_{abr} \cdot \Delta MRR_{abr} \quad (8)$$

Archard wear model was proposed to describe sliding wear based on the theory of friction contact mechanics [101]. The total wear volume is given by Eq. (9).

$$V = K_{arc} s \frac{P}{H} \quad (9)$$

where  $V$  is the total wear volume,  $s$  is the sliding distance,  $K_{arc}$  is the wear coefficient,  $p$  is the total normal load, and  $H$  is the hardness of the softest contacting surfaces. According to Archard wear equation, mathematical model of  $MRR$  in any time  $t$  can be described by Eq. (10).

$$MRR = \rho dV/dt \quad (10)$$

where  $\rho$  is the density of the workpiece.

Li et al. [27] developed a mathematic model of MRR as a function of magnetic flux density, mass ratio, rotational speed of magnetic poles, rotational speed of cam, and diameter of abrasive particles and ferromagnetic particles. The relative error between experimental values and predicted values was 4.51 %. Tian et al. [102] built a theoretical model for material removal intensity to achieve an optimal position for workpiece fixing onto the wall of vibratory bowl to obtain high-efficiency finishing. For the study of other MRR calculation methods, Zhang et al. [103] explored MRR in mg/min applying Eq. (11).

$$\begin{cases} V = NAL \\ MRR = pV/t \end{cases} \quad (11)$$

where  $N$  is the number of active abrasives,  $A$  is the area of indentation cross section, and  $L$  is the Length of workpiece.

Among them, the calculated method of active abrasives was a related function of length of top magnet and diameter of abrasive, and area of indentation cross-section was obtained based the model of indentation cross-section [104]. The predicted MRR was in good agreement with the measured data obtained by experiments. Ma et al. [105] predicted the MRR model as a function of the cross-sectional area cutting into workpiece, feed rate of magnetic abrasive, the density of the workpiece, and finishing time. The predicted MRR model is combined with experiments to analyze the processed surface morphology, roughness, residual stress, etc.

## 7 Challenges and future directions

Although MAF process has achieved much technical advancement in recent years, there are a lot of challenges and potentials that need to be explored.

- MAF principles with high efficiency and strong controllability are developed for the microstructure surface and difficult-to-finish materials. At present, difficult-to-finish materials such as titanium alloys, high-speed steel, glasses, ceramics, and composites have attracted extensive attention. MAF is still insufficient in finishing parts with the microstructure surface made of difficult-to-finish materials, such as gears, impellers, complex molds, etc., resulting in poor uniformity and low efficiency. MAF technology need to be further explored to solve the weakness.
- Magnetic abrasive with high performance and low cost needs to be further developed. The performance of magnetic abrasive is the critical factor affecting the finishing efficiency and the desired improvement in surface quality. Developments of reasonable magnetic abrasive is a key issue to obtain high-quality surfaces and improve the material removal rate. It is necessary to prepare suitable magnetic abrasive considering shear capacity, high saturation magnetization, dispersibility, and properties. Therefore, solution of weakness needs to be paid attention.
- A controllable magnetic finishing equipment with feedback function, a real-time monitoring system, and online inspection are necessary to be further investigated. At present, it is mainly to perform offline inspection on the processed workpiece to determine the finishing quality, which will affect the finishing efficiency, the automatic compensation accuracy of the workpiece, and the surface quality of the workpiece to a certain extent. Therefore, the development of intelligent magnetic abrasive equipment with feedback, a real-time monitoring system and online inspection is one of the challenges and future directions, which is able to realize automation finishing and the compensation of finishing parameters.

- Magnetic field simulation of the MAF equipment. Simulations in existing scientific literatures mainly focused on magnetic field generation tools. Simulation results exist a large error comparing with the actual finishing magnetic field environment. Magnetic field simulation including magnetic field generation tools, fixtures, workpiece, magnetic abrasive, and automation equipment is necessary to obtain more information on real magnetic field strength.
- Establish a universal and accurate MRR model system considering the interaction of magnetic abrasive's composition. The mechanism for the media formation and its interaction with the workpiece surface is complex, so some assumptions are made to simplify the mathematical modelling of MRR model. MRR model is mainly established based on Preston equation, which divides the pressure on the workpiece into several parts. Therefore, it is significant to establish a universal mathematical model for MRR.

## 8 Conclusions

This paper presented an overview of research advances in MAF process. It can be summarized as follows:

- MAF is a nano-finishing technology. The micro-cutting is realized by providing magnetic pole rotation and workpiece reciprocating motion, in which magnetic abrasive is a cutting tool.
- Magnetic abrasive is mainly prepared by simply mixing method, bonding method, sintering method, gas atomization, and rapid solidification method.
- The great majority of MAF tools are designed using permanent magnets rather than electromagnetic coils to avoid the disadvantage of eddy current heat and magnetic field strength shortage.
- MAF modeling and simulation are established to predict optimal processing parameters in achieving the desired improvement in workpiece and reduce multiple experiments.
- The finishing efficiency based on the given input process parameters are predicted by MRR model. The calculation of pressure is usually the superposition of several parts of pressure, which does not give a unified model.

**Acknowledgments** The authors gratefully acknowledge financial supports by the National Natural Science Foundation of China (Grant No. 51875329 and 51905323), Taishan Scholar Special Foundation of Shandong Province (Grant No. tsqn201812064), Shandong Provincial Natural Science Foundation, China (Grant No. ZR2017MEE050), Shandong Provincial Key Research and Development Project, China (Grant No. 2018GGX103008), Scientific Innovation Project for Young

Scientists in Shandong Provincial Universities (Grant No. 2019KJB030), and Key Research and Development Project of Zibo City (Grant No. 2019ZBXC070).

## References

1. Guo DM, Sun YW, Jia ZY (2014) Methods and research progress of high-performance manufacturing. *J Mech Eng* 50(11):119–134. <https://doi.org/10.3901/JME.2014.11.119>
2. Heo JS, Koo Y, Choi SS (2004) Grinding characteristics of conventional and ELID methods in difficult-to-cut and hardened brittle materials. *J Mater Process Technol* 155–156:1196–1200. <https://doi.org/10.1016/j.jmatprotec.2004.04.394>
3. Evans CJ, Paul E, Dornfeld D, Lucca DA, Byrne G, Tricard M, Klocke F (2003) Material removal mechanisms in lapping and polishing. *CIRP Ann* 52(2):611–633. [https://doi.org/10.1016/S0007-8506\(07\)60207-8](https://doi.org/10.1016/S0007-8506(07)60207-8)
4. Dubey AK, Shan HS, Jain NK (2008) Analysis of surface roughness and out-of-roundness in the electro-chemical honing of internal cylinders. *Int J Adv Manuf Technol* 38(5–6):491–500. <https://doi.org/10.1007/s00170-007-1180-z>
5. Houshi MN (2016) A Comprehensive review on magnetic abrasive finishing process. *Adv Eng Forum* 18:1–20. <https://doi.org/10.4028/www.scientific.net/AEF.18.1>
6. Kumari C, Chak SK (2018) A review on magnetically assisted abrasive finishing and their critical process parameters. *Manuf Rev* 5(13):1–16. <https://doi.org/10.1051/mfreview/2018010>
7. Jha S, Jain VK (2006) Nano finishing Techniques. In: *Micromanufacturing and Nanotechnology*. Springer, Berlin, pp 171–195
8. Mori Y, Ikawa N, Sugiyama K (1978) Elastic emission machining. Stress field and fracture mechanism. *Technology Reports of the Osaka University* 28(1430–1458):525–532
9. Spencer EG, Schmidt PH (1971) Ion-Beam Techniques for Device Fabrication. *J Vac Sci Technol* 8(5):52–70. <https://doi.org/10.1116/1.1316390>
10. Kim TW, Kang DM, Kwak JS (2010) Application of magnetic abrasive polishing to composite materials. *J Mech Sci Technol* 24(5):1029–1034. <https://doi.org/10.1007/s12206-010-0323-6>
11. Du ZW, Chen Y, Zhou K, Li C (2015) Research on the electrolytic-magnetic abrasive finishing of nickel-based superalloy GH4169. *Int J Adv Manuf Technol* 81(5–8):897–903. <https://doi.org/10.1007/s00170-015-7270-4>
12. Zou Y, Xie HJ, Dong CW, Wu JZ (2018) Study on complex micro surface finishing of alumina ceramic by the magnetic abrasive finishing process using alternating magnetic field. *Int J Adv Manuf Technol* 97(5–8):2193–2202. <https://doi.org/10.1007/s00170-018-2064-0>
13. Vahdati M, Sadeghinia E, Shokuhfar A (2010) Magnetic assisted abrasion, a new method for nano level surface finishing. *Diffus Defect Forum* 297–301:402–407. <https://doi.org/10.4028/www.scientific.net/ddf.297-301.402>
14. Chang GW, Yan BH, Hsu RT (2002) Study on cylindrical magnetic abrasive finishing using unbonded magnetic abrasive. *Int J Mach Tools Manuf* 42(5):575–583. [https://doi.org/10.1016/S0890-6955\(01\)00153-5](https://doi.org/10.1016/S0890-6955(01)00153-5)
15. Wang AC, Tsai L, Lin YC, Wu KL (2013) Evaluation of rheological properties of gel abrasive in magnetic abrasive finishing. *Adv Mech Eng* 2013:1–7. <https://doi.org/10.1155/2013/493780>
16. Niknam SA, Davoodi B, Davim P, Songmene V (2018) Mechanical deburring and edge-finishing processes for aluminum parts—a review. *Int J Adv Manuf Technol* 95:1101–1125. <https://doi.org/10.1007/s00170-017-1288-8>

17. Yan BH, Chang GW, Cheng TJ, Hsu RT (2003) Electrolytic magnetic abrasive finishing. *Int J Mach Tools Manuf* 46(13):1355–1366. [https://doi.org/10.1016/S0890-6955\(03\)00151-2](https://doi.org/10.1016/S0890-6955(03)00151-2)
18. Kanish TC, Narayanan S, Kuppan P, Ashok SD (2017) Investigations on the finishing forces in magnetic field assisted abrasive finishing of SS316L. *Procedia Eng* 174:611–620. <https://doi.org/10.1016/j.proeng.2017.01.196>
19. Ganguly V, Schmitz T, Graziano A, Yamaguchi H (2013) Force measurement and analysis for magnetic field-assisted finishing. *J Manuf Sci Eng* 135(4):041016. <https://doi.org/10.1115/1.4023723>
20. Singh RK, Singh DK, Gangwar S (2018) Advances in magnetic abrasive finishing for futuristic requirements - a review. *Mater Today Proc* 5(9):20455–20463. <https://doi.org/10.1016/j.matpr.2018.06.422>
21. Heng L, Kim YJ, Mun SD (2017) Review of superfinishing by the magnetic abrasive finishing process. *High Speed Mach* 3(1):42–55. <https://doi.org/10.1515/hsm-2017-0004>
22. Yamaguchi H, Shinmura T (2004) Internal finishing process for alumina ceramic components by a magnetic field assisted finishing process. *Precis Eng* 28(2):135–142. <https://doi.org/10.1016/j.precisioneng.2003.07.001>
23. Barman A, Das M (2018) Simulation and experimental investigation of finishing forces in magnetic field assisted finishing process. *Mater Manuf Process* 33(11):1223–1232. <https://doi.org/10.1080/10426914.2018.1453157>
24. Mulik RS, Pandey PM (2011) Ultrasonic assisted magnetic abrasive finishing of hardened AISI 52100 steel using unbonded SiC abrasive. *Int J Refract Met Hard Mater* 29(1):68–77. <https://doi.org/10.1016/j.ijmhm.2010.08.002>
25. Zhou K, Chen Y, Du ZW, Niu FL (2015) Surface integrity of titanium part by ultrasonic magnetic abrasive finishing. *Int J Adv Manuf Technol* 80(5-8):997–1005. <https://doi.org/10.1007/s00170-015-7028-z>
26. Zhang GX, Zhao YG, Zhao DB, Yin FS, Zhao ZD (2011) Preparation of white alumina spherical composite magnetic abrasive by gas atomization and rapid solidification. *Scr Mater* 65(5):416–419. <https://doi.org/10.1016/j.scriptamat.2011.05.021>
27. Li WH, Li XH, Yang SQ, Li WD (2018) A newly developed media for magnetic abrasive finishing process: material removal behavior and finishing performance. *J Mater Process Technol* 260:20–29. <https://doi.org/10.1016/j.jmatprotec.2018.05.007>
28. Chen Y, Song QH, Wang X (2007) Study on the characteristics of simply mixed the magnetic abrasive particles. *Adv Mater Res* 24-25:133–138. <https://doi.org/10.4028/www.scientific.net/AMR.24-25.133>
29. Ahn BW, Lee SH (2012) Run-to-run process control of magnetic abrasive finishing using bonded abrasive particles. *Proc Inst Mech Eng B J Eng Manuf* 226(12):1963–1975. <https://doi.org/10.1177/0954405412462318>
30. Liao GB, Zhang MM, Li YJ, Liu ZQ, Chen Y (2011) Preparation of magnetic abrasive by sintering method finishing by sintering method. *Key Eng Mater* 487:273–277. <https://doi.org/10.4028/www.scientific.net/kem.487.273>
31. Chen Y, Zhang MM, Liu ZQ (2011) Study on sintering process of magnetic abrasive particles. *Adv Mater Res* 337:163–167. <https://doi.org/10.4028/www.scientific.net/amr.337.163>
32. Chen HL, Li WH, Yang SQ, Yang SC (2010) Research of magnetic abrasive prepared by hot pre-sintering process. In: 2010 5th IEEE Conference on Industrial Electronics and Applications, Taichung, pp 776–778. <https://doi.org/10.1109/ICIEA.2010.5516736>
33. Zhao ZD, Huang YH, Zhao YG (2010) Preparation of magnetic abrasive by sintering method. *Adv Mater Res* 135:382–387. <https://doi.org/10.4028/www.scientific.net/amr.135.382>
34. Hu B, Lu YP (2012) Study on preparation technology and finishing performance of magnetic abrasive grain. *Adv Mater Res* 452-453:637–641. <https://doi.org/10.4028/www.scientific.net/amr.452-453.637>
35. Gao YG, Zhao YG, Zhang GG (2018) Preparation of Al<sub>2</sub>O<sub>3</sub> magnetic abrasive by gas-solid two-phase double-stage atomization and rapid solidification. *Mater Lett* 215:300–304. <https://doi.org/10.1016/j.matlet.2017.12.124>
36. Yang LD, Lin CT, Chou HM (2009) Optimization in MAF operations using Taguchi parameter design for AISI304 stainless steel. *Int J Adv Manuf Technol* 59(42):595–605. <https://doi.org/10.1007/s00170-008-1612-4>
37. Shukla VC, Pandey PM, Dixit US, Roy A, Silberschmidt V (2017) Modeling of normal force and finishing torque considering shearing and ploughing effects in ultrasonic assisted magnetic abrasive finishing process with sintered magnetic abrasive powder. *Wear* 15(390-191):11–22. <https://doi.org/10.1016/j.wear.2017.06.017>
38. Qin P, Zhang GX, Zhao YG, Jiang LZ, Teng X, Liang JP (2020) Study of CBN/Fe-based spherical magnetic abrasive bonding interfacial microstructure prepared by gas atomization with rapid solidification. *Adv Powder Technol* 31(4):1597–1602. <https://doi.org/10.1016/j.apt.2020.01.036>
39. Fan ZH, Tian YB, Zhou Q, Shi C (2020) Enhanced magnetic abrasive finishing of Ti-6Al-4V using shear thickening fluids additives. *Precis Eng* 64:300–306. <https://doi.org/10.1016/j.precisioneng.2020.05.001>
40. Kanish TC, Narayanan S, Kuppan P, Denis AS (2018) Investigations on wear behavior of magnetic field assisted abrasive finished SS316L material. *Mater Today Proc* 5(5):12734–12743. <https://doi.org/10.1016/j.matpr.2018.02.257>
41. Kwak JS (2009) Enhanced magnetic abrasive polishing of non-ferrous metals utilizing a permanent magnet. *Int J Mach Tools Manuf* 49(7-8):613–618. <https://doi.org/10.1016/j.ijmachtools.2009.01.013>
42. Kala P, Pandey PM, Verma GC, Sharma V (2017) Understanding flexible abrasive brush behavior for double disk magnetic abrasive finishing based on force signature. *J Manuf Process* 28(3):442–448. <https://doi.org/10.1016/j.jmappro.2017.04.010>
43. Laroux KG (2008) Using magnetic abrasive finishing for deburring produces parts that perform well and look great. *Alluring and Deburring*. <https://www.yumpu.com/en/document/read/11479441>. Accessed 17 June 2020
44. Sato T, Kum CW, Venkatesh VC (2013) Rapid magnetorheological finishing of ti-6al-4v for aerospace components. *Int J Nanomanuf* 9(5/6):431. <https://doi.org/10.1504/IJNM.2013.057590>
45. Fan ZH, Tian YB, Liu ZQ, Shi C, Zhao YG (2019) Investigation of a novel finishing tool in magnetic field assisted finishing for titanium alloy Ti-6Al-4V. *J Manuf Process* 43:74–82. <https://doi.org/10.1016/j.jmappro.2019.05.007>
46. Tian YB, Shi C, Fan ZH, Zhou Q (2020) Experimental investigations on magnetic abrasive finishing of ti-6al-4v using a multiple pole-tip finishing tool. *Int J Adv Manuf Technol* 106:3071–3080. <https://doi.org/10.1007/s00170-019-04871-z>
47. Jain NK, Jain VK, Jha S (2006) Parametric optimization of advanced fine-finishing processes. *Int J Adv Manuf Technol* 34(11-12):1191–1213. <https://doi.org/10.1007/s00170-006-0682-4>
48. Xie HJ, Zou YH, Dong CW, Wu JZ (2019) Study on the magnetic abrasive finishing process using alternating magnetic field: investigation of mechanism and applied to aluminum alloy plate. *Int J Adv Manuf Technol* 102(5-8):1509–1520. <https://doi.org/10.1007/s00170-018-03268-8>
49. Yang SQ, Li WH (2018) Surface finishing theory and new technology. Heidelberg, Berlin

50. Shinmura T, Takazawa K, Hatano E, Matsunaga M, Matsuo T (1990) Study on magnetic abrasive finishing. *CIRP Ann* 39(1): 325–328. [https://doi.org/10.1016/s0007-8506\(07\)61064-6](https://doi.org/10.1016/s0007-8506(07)61064-6)
51. Yamaguchi H, Shinmura T (1996) Study on a new internal finishing process by the application of magnetic abrasive machining. *Int J Jpn Soc Precis Eng* 62(11):1617–1621. <https://doi.org/10.2493/jjspe.62.1617>
52. Shinmura T, Yamaguchi H (1995) Study on a new internal finishing process by the application of magnetic abrasive machining internal finishing of stainless-steel tube and clean gas bomb. *JSME International Journal. Ser C, Dynamics, Control, Robotics, Design And Manufacturing* 38(4):798–804. <https://doi.org/10.1299/jsmec1993.38.798>
53. Yamaguchi H, Shinmura T (1999) Study of the surface modification resulting from an internal magnetic abrasive finishing process. *Wear* 225–229:246–255. [https://doi.org/10.1016/s0043-1648\(99\)00013-7](https://doi.org/10.1016/s0043-1648(99)00013-7)
54. Yamaguchi H, Shinmura T, Takenaga M (2003) Development of a new precision internal machining process using an alternating magnetic field. *Precis Eng* 27(1):51–58. [https://doi.org/10.1016/s0141-6359\(02\)00177-0](https://doi.org/10.1016/s0141-6359(02)00177-0)
55. Sato T, Yamaguchi H, Shinmura T (2007) Study of internal magnetic field assisted finishing for copper tubes with MRF (Magneto-rheological Fluid)-based Slurry. *Key Eng Mater* 329:249–254. <https://doi.org/10.4028/www.scientific.net/KEM.329.249>
56. Singh P, Samra PS, Singh L (2011) Internal finishing of cylindrical pipes using sintered magnetic abrasive. *Int J Eng Sci Technol* 3:5474–5753 [www.researchgate.net/publication/267566264](http://www.researchgate.net/publication/267566264). Accessed 17 Jan 2020
57. Wang D, Shinmura T, Yamaguchi H (2004) Study of magnetic field assisted mechanochemical polishing process for inner surface of Si3N4 ceramic components. *Int J Mach Tools Manuf* 44(14): 1547–1553. <https://doi.org/10.1016/j.ijmactools.2004.04.024>
58. Li XH (2010) Theoretical analysis and experimental study on hole surface finishing new technology based on magnetic field characteristics. Dissertation, Taiyuan University of Technology
59. Kang J, Yamaguchi H (2012) Internal finishing of capillary tubes by magnetic abrasive finishing using a multiple pole-tip system. *Precis Eng* 36(3):510–516. <https://doi.org/10.1016/j.precisioneng.2012.01.006>
60. Shanbhag VV, Naveen K, Balashanmugam N, Vinod P (2016) Modelling for evaluation of surface roughness in magnetic abrasive finishing of flat surfaces. *Int J Precis Technol* 6(2):159–170. <https://doi.org/10.1504/IJPTTECH.2016.078190>
61. Lu A, Jin T, Liu Q, Guo Z, Qu M, Luo H, Han M (2019) Modeling and prediction of surface topography and surface roughness in dual-axis wheel polishing of optical glass. *Int J Mach Tools Manuf* 137:13–29. <https://doi.org/10.1016/j.ijmactools.2018.10.001>
62. Mosavat M, Rahimi A (2019) Simulation and experimental study on the effect of abrasive size, rotational speed, and machining gap during ultra-precision polishing of monocrystalline silicon. *Colloids Surf A Physicochem Eng Asp* 575(20):50–56. <https://doi.org/10.1016/j.colsurfa.2019.05.005>
63. Jain VK, Jayswal SC, Dixit PM (2007) Modeling and Simulation of Surface Roughness in Magnetic abrasive finishing Using Non-Uniform Surface Profiles. *Mater Manuf Process* 22(2):256–270. <https://doi.org/10.1080/10426910601134096>
64. Kajal S, Jain VK, Ramkumar J, Nagdeve L (2017) Experimental and theoretical investigations into internal magnetic abrasive finishing of a revolver barrel. *Int J Adv Manuf Technol* 100: 1105–1122. <https://doi.org/10.1007/s00170-017-1220-2>
65. Kala P, Pandey PM (2015) Comparison of finishing characteristics of two paramagnetic materials using double disc magnetic abrasive finishing. *J Manuf Process* 17:63–77. <https://doi.org/10.1016/j.jmapro.2014.07.007>
66. Kala P, Sharma V, Pandey PM (2017) Surface roughness modelling for double disk Magnetic abrasive finishing process. *J Manuf Process* 25:37–48. <https://doi.org/10.1016/j.jmapro.2016.10.007>
67. Yun H, Han B, Chen Y, Liao M (2015) Internal finishing process of alumina ceramic tubes by ultrasonic-assisted magnetic abrasive finishing. *Int J Adv Manuf Technol* 85(1–4):727–734. <https://doi.org/10.1007/s00170-015-7927-z>
68. Jiao AY, Quan HJ, Li ZZ, Zou YH (2015) Study on improving the trajectory to elevate the surface quality of plane magnetic abrasive finishing. *Int J Adv Manuf Technol* 80(9–12):1613–1623. <https://doi.org/10.1007/s00170-015-7136-9>
69. Jayswal SC (2004) Analysis of magnetic abrasive finishing with slotted magnetic pole. *AIP Conf Proc* 721(1):1435–1440. <https://doi.org/10.1063/1.1766730>
70. Srinivas K, Murtaza Q, Aggarwal AK (2019) Effect of shape of magnet on the machining of workpiece. *Int J Technol Eng* 8(2S11):2909–2913. <https://doi.org/10.35940/ijrte.B1367.0982S1119>
71. Zhao YG, Jiang YC, Zhou JJ (1999) Study on the influence of the shape and size of the magnetic pole slot on the magnetic field distribution and the magnetic particle finishing ability. *China Mech Eng* 06:93–96 <https://doi.org/CNKI:SUN:ZGJX.0.1999-06-027>
72. Yin SH, Zhu KJ, Fan YF, Zhu YJ, Chen Y, Wang Y (2010) Influences of polishing tool's shape on surface roughness in magneto-rheological finishing. *Adv Mater Res* 97–101:4092–4095. <https://doi.org/10.4028/www.scientific.net/AMR.97-101.4092>
73. Liu WY, Zhang GX (2013) Design and simulation of plane magnet pole on magnetic abrasive finishing. *Mod Manuf Eng* 7:76–81 <https://doi.org/CNKI:SUN:XXGY.0.2013-07-017>
74. Zhao WC, Zhang GX, Chen CZ (2016) Design and simulation research of the magnetic poles' structure parameters on magnetic abrasive finishing system. *Mach Des Res* 32(06):106–109 <https://doi.org/CNKI:SUN:JSYY.0.2016-06-030>
75. Zhang P, Zhang G, Liang W, Qin P, Jiang L (2018) Research on magnetic abrasive finishing processes of aluminum-magnesium alloy permanent magnet poles. *China Mech Eng* 29(11):1324–1328. <https://doi.org/10.3969/j.issn.1004-132X.2018.11.011>
76. Mishra V, Goel H, Mulik RS, Pandey PM (2014) Determining work-brush interface temperature in magnetic abrasive finishing process. *J Manuf Process* 16(2):248–256. <https://doi.org/10.1016/j.jmapro.2013.10.004>
77. Wang R, Park JH, Heng L, Kim Y, Jeong JY, Mun SD (2018) Effect of temperature on the magnetic abrasive finishing process of Mg alloy bars. *J Mech Sci Technol* 32(5):2227–2235. <https://doi.org/10.1007/s12206-018-0433-0>
78. Singh RK, Gangwar S, Singh DK (2019) Experimental investigation on temperature-affected magnetic abrasive finishing of aluminum 6060. *Mater Manuf Process* 34(11):1274–1285. <https://doi.org/10.1080/10426914.2019.1628263>
79. Mosavat M, Rahimi A (2019) Numerical-experimental study on polishing of silicon wafer using magnetic abrasive finishing process. *Wear* 424–425:143–150. <https://doi.org/10.1016/j.wear.2019.02.007>
80. Jayswal SC, Jain VK, Dixit PM (2005) Modeling and simulation of magnetic abrasive finishing process. *Int J Adv Manuf Technol* 26(5–6):477–490. <https://doi.org/10.1007/s00170-004-2180-x>
81. Madhab GB, Jain VK, Dixit PM (2006) On simulation of magnetic abrasive finishing process for plane surfaces using FEM. *Int J Mach Mach Mater* 1(2):133–165. <https://doi.org/10.1504/ijmmm.2006.011063>
82. Judal KB, Yadava V (2014) Modeling and Simulation of Cylindrical Electrochemical Magnetic Abrasive Machining Process. *Mach Sci Technol* 18(2):221–250. <https://doi.org/10.1080/10910344.2014.897841>

83. Judal KB, Yadava V (2012) Experimental investigations into cylindrical electro-chemical magnetic abrasive machining of AISI-420 magnetic stainless steel. *Int J Abras Technol* 5(4):315–331. <https://doi.org/10.1504/ijat.2012.052039>
84. Kim JD, Choi MS (1995) Simulation for the prediction of surface-accuracy in magnetic abrasive machining. *J Mater Process Technol* 53(3–4):630–642. [https://doi.org/10.1016/0924-0136\(94\)01753-n](https://doi.org/10.1016/0924-0136(94)01753-n)
85. Kim JD, Choi MS (1997) Study on magnetic polishing of free-form surfaces. *Int J Mach Tools Manuf* 37(8):1179–1187. [https://doi.org/10.1016/s0890-6955\(95\)00078-x](https://doi.org/10.1016/s0890-6955(95)00078-x)
86. Mori T, Hirota K, Kawashima Y (2003) Clarification of magnetic abrasive finishing mechanism. *J Mater Process Technol* 143–144: 682–686. [https://doi.org/10.1016/s0924-0136\(03\)00410-2](https://doi.org/10.1016/s0924-0136(03)00410-2)
87. Singh DK, Jain VK, Raghuram V (2004) Parametric study of magnetic abrasive finishing process. *J Mater Process Technol* 149(1–3):22–29. <https://doi.org/10.1016/j.jmatprotec.2003.10.030>
88. Singh DK, Jain VK, Raghuram V (2005) Experimental investigations into forces acting during a magnetic abrasive finishing process. *Int J Adv Manuf Technol* 30(7–8):652–662. <https://doi.org/10.1007/s00170-005-0118-6>
89. Preston FW (1927) The theory and design of plate glass polishing machines. *J Soc Glas Technol* 11:214–256
90. Buijs M, Houten KV (1993) A model for lapping of glass. *J Mater Sci* 28(11):3014–3020. <https://doi.org/10.1007/BF00354706>
91. DeGroote JE, Marino AE, Wilson JP, Bishop AL, Lambropoulos JC, Jacobs SD (2007) Removal rate model for magnetorheological finishing of glass. *Appl Opt* 46(32):7927–7941. <https://doi.org/10.1364/ao.46.007927>
92. Yin SH (2009) Magnetic field assisted ultra-precision finishing. Hunan University Press, Hunan, pp 16–21
93. Chen F, Yin S, Yu J, Xu Z (2011) New progresses on magnetorheological finishing (MRF) technology. *China Mech Eng* 22(19):2382–2239. <https://doi.org/CNKI:SUN:ZGJX.0.2011-19-023>
94. Wani AM, Yadava V, Khatri A (2007) Simulation for the prediction of surface roughness in magnetic abrasive flow finishing (MAFF). *J Mater Process Technol* 190(1–3):282–290. <https://doi.org/10.1016/j.jmatprotec.2007.02.036>
95. Zhang F, Zhang XJ (2000) Yu J (2000) Mathematics model of magnetorheological finishing. *Adv Opt Manuf Test Technol*. <https://doi.org/10.1117/12.402796>
96. Chen FJ, Yin SH, Ohmori H (2008) Two-dimension modelling for material removal of magneto-rheological finishing. *China Mech Eng* 20(14):1647–1650
97. Li YM, Shen XQ, Wang AL (2010) Research on material removal modeling and processing parameters of magnetorheological finishing. *Adv Mater Res* 102–104:746–749. <https://doi.org/10.4028/www.scientific.net/AMR.102-104.746>
98. Misra AM, Pandey P, Dixit US (2017) Modeling of material removal in ultrasonic assisted magnetic abrasive finishing process. *Int J Mech Sci* 131–132:853–867. <https://doi.org/10.1016/j.ijmecsci.2017.07.023>
99. Yuan JL, MAO MJ, Li M, Liu S, Hu ZH, Wu F (2019) Chemical and mechanical polishing mechanism of cemented carbide tool material. *Surf Technol* 48(2):260–267. <https://doi.org/10.16490/j.cnki.issn.1001-3660.2019.02.037>
100. Kum CW, Sato T, Guo J, Liu K, Butler D (2018) A novel media properties-based material removal rate model for magnetic field-assisted finishing. *Int J Mech Sci* 141:189–197. <https://doi.org/10.1016/j.ijmecsci.2018.04.006>
101. Archard JF (1953) Contact and Rubbing of Flat Surfaces. *J Appl Phys* 24(8):981–988. <https://doi.org/10.1063/1.1721448>
102. Tian YB, Zhong ZW, Tan SJ (2016) Kinematic analysis and experimental investigation on vibratory finishing. *Int J Adv Manuf Technol* 86(9–12):3113–3121. <https://doi.org/10.1007/s00170-016-8378-x>
103. Zhang J, Chaudhari A, Wang H (2019) Surface quality and material removal in magnetic abrasive finishing of selective laser melted 316 L stainless steel. *J Manuf Process* 45:710–719. <https://doi.org/10.1016/j.jmapro.2019.07.044>
104. Weisstein E (2019) Circular segment. <https://mathworld.wolfram.com/CircularSegment.html>. Accessed 17 June 2020
105. Ma FJ, Luan SY, Luo QC (2019) Effects of ultrasonic assisted magnetic abrasive finishing on surface integrity of titanium alloy. *China Surf Eng* 32(02):128–136. <https://doi.org/10.11933/j.issn.1007-9289.20181105001>

**Publisher's note** Springer Nature remains neutral with regard to jurisdictional claims in published maps and institutional affiliations.